ISSN 2347-3487

Effect of aluminum content on structure, transport and mechanical properties of Sn-Zn eutectic lead free solder alloy rapidly solidified from melt.

Rizk Mostafa Shalaby[1,*], Mohamed Munther[1,2], Abu-Bakr Al-Bidawi[1], Mustafa Kamal[1].
[1] Metal Physics Laboratory, Physics Department, Faculty of Science, Mansoura University, Mansoura, P.O.Box: 35516, Mansoura, Egypt.
College of Science, University of AL-Anbar, Iraq

Abstract

The greatest advantage of Sn-Zn eutectic is its low melting point (198 °C) which is close to the melting point. of Sn-Pb eutectic solder (183 °C), as well as its low price per mass unit compared with Sn-Ag and Sn-Ag-Cu solders. In this paper, the effect of 0.0, 1.0, 2.0, 3.0, 4.0, and 5.0 wt. % Al as ternary additions on melting temperature, microstructure, microhardness and mechanical properties of the Sn-9Zn lead-free solders were investigated. It is shown that the alloying additions of Al at 4 wt. % to the Sn-Zn binary system lead to lower of the melting point to 195.72 °C. From x-ray diffraction analysis, an aluminium phase, designated α-Al is detected for 4 and 5 wt. % Al compositions. The formation of an aluminium phase causes a pronounced increase in the electrical resistivity and microhardness. The ternary Sn-9Zn-2 wt.%Al exhibits micro hardness superior to Sn-9Zn binary alloy. The better Vickers hardness and melting points of the ternary alloy is attributed to solid solution effect, grain size refinement and precipitation of Al and Zn in the Sn matrix. The Sn-9%Zn-4%Al alloy is a lead-free solder designed for possible drop-in replacement of Pb-Sn solders.

Keywords

lead free solder; Sn-Zn-Al; Microstructure; Rapid solidification; Thermal properties; Mechanical properties

ISSN 2347-3487

Introduction

The intent of this study is to continue and to describe the effect of aluminum content on structure and solder properties of Sn-Zn eutectic [1]. It is well known that lead and lead-containing materials are toxic and dangerous to the surrounding environment. Among Pb-free alternatives to traditional solders, Sn-9Zn eutectic alloy has the closest melting point (melting temperature ~ 471 K) to the Sn-40Pb solder (melting temperature ~ 456 K), much lower compared to broadly used Sn-Ag-Cu (SAC) solder (melting temperature ~ 490 K). This is quite important as the low soldering temperatures reduces possible heat damage to joined elements. Also the temperature range could be broadened in the case of step-soldering process. Sn-Zn-Al ternary system is studied with the world-wide search for materials which play important role in high temperature lead free soldering for applications in electrical engineering and in automotive industry [2, 3]. The presence of Al is very important because of low toxicity in comparison with the alloys containing lead, of the increased anti-corrosion effects caused by the presence of Al, and also other properties , such as wettability, structural, and electrical conductivity. Electrical resistivity and thermal expansion of Sn-Zn-In alloys had studied by Tomasz Gancarz et al [4]. They reported that the electrical resistivity of alloys increases linearly with temperature and concentration of indium. Also, scanning electron microscopy revealed simple eutectic microstructure with In dissolved in Sn-rich matrix. Microstructure and interfacial reaction of Sn-Zn-x(Al, Ag) near eutectic solders on Al and Cu substrates had studied by M.L.Huang et al [5]. Effect of indium content and rapid solidification on microhardness and micro-creep of Sn-Zn eutectic lead free solder alloy had studied by R M Shalaby [6]. He is concluded that the alloying additions of indium to the Sn-Zn binary system result in a reducing the melting point to 187.9 ˚C and at the same time significantly improve the crystalline size. Several papers discussed wettability , oxidation resistance, melting , mechanical properties, and microstructures of Sn-Zn based solders and interfaces with Cu and Ni substrates, a great number of them was reviewed by Zhang et al. [7]. McCormack et al. [8] were the first to propose Sn-Zn-In solder. They found the melting temperature of Sn-Zn-5In (wt.%) 10 K lowers than 471 K of Sn-9Zn and wetting behavior improved compared to Sn-9Zn solder. Recently, Sn-Zn solder has become highly recommended as a substitute for Sn-Pb eutectic solder due to its lower melting point [9-12]. Sn-Zn solder can also be used without replacing the existing manufacturing lines or electronic components [13]. Moreover, Sn-Zn is advantageous from an economic point-of-view because Zn is a law cost metal. However, Sn-Zn eutectic solder is difficult to handle practically due to its highly active characteristics. The basic microstructures of Sn-9Zn binary alloys and their interfaces with Cu and Ni were investigated [13-15]. For electronic parts and devices, solder joints provide electrical conductivity and suitable mechanical strength [16, 17]. So that the aim of the present work to study effect of aluminum content on structure, transport and mechanical properties of Sn-Zn eutectic lead free solder alloy rapidly solidified from molten state.

2 . Experimental Procedures

The experimental techniques utilized have been described in details [18-21] and will be repeated here only briefly. The materials used in the present work are Sn, Zn, and Al granules, and the starting purity was 99.99%. Sn-Zn_9-Alx (where X were varying from 1.0 to 5 wt. %) quenched from melt ribbons have been produced by a single aluminum roller coated with copper (200mm in diameter) melt-spinning technique [22]. The process parameters such as, the ejection temperature and the linear speed of the wheel were fixed at 550 k and 30.4 ms^{-1} respectively. The material flow rate of has been empirically found to be an important chill block melt-spin process variable and its dependence on readily adjustable apparatus parameters has been described by Liebermann [23]. In the present study this parameter is calculated from:

$$Q_f = V_r W t \quad \dots\dots\dots\dots.(1)$$

Where (Vr) is the ribbon or substrate velocity, (W) is the ribbon width and (t) the average thickness calculated by dividing the ribbon mass (m) by length (l), density (ρ) and width (W).

$$t = \frac{m}{lw\rho} \quad \dots\dots\dots\dots.(2)$$

X-ray diffraction analysis was done on a Shimadzu x-ray diffractometer (DX-30), using Cu kα radiation (λ=1.5406 Å) with Ni-filter. The microstructure analysis was carried out on a scanning electron microscope (SEM) of type (JEOL JSM-6510LV, Japan) operate at 30 KV with high resolution 3 nm. Differential thermal analysis (DTA) was carried out on a (SDT Q600, USA) with a heat rate 10 C min^{-1}.The temperature dependence of resistivity was carried out by the double-bridge methods [24]. The variation of temperature during the resistance temperature investigation was determined using a step-down transformer connected to a constructed temperature control. The heating was kept constant during all the investigations at 5 K.min^{-1} [22]. The elastic moduli, the internal friction and the thermal diffusivity of melt-spun ribbons were examined in air atmosphere with a modified dynamic resonance method [25]. The hardness of the melt-spun ribbons was measured using a digital Vickers microhardness tester (model FM-7), applying a load of 10 gf for 5 sec via a Vickers diamond pyramid [26].

3. Results and Discussions

3.1 Structural analysis

The XRD patterns of melt spun ribbons are shown in Fig. 1. The diffraction pattern of eutectic Sn-9Zn alloy indexed with a majority of β-Sn body centered tetragonal phase and secondary Zn hexagonal phase, implying successful alloying of Sn and Zn during melt spun process. No prominent oxide peak was observed in the diffraction measurements. Fig.1b shows the XRD profiles of the Sn-9Zn- 1 wt.% Al melt spun alloys. The obtained phases are the same present in Fig.1a. It is well know that the dissolved Al in solder matrix Sn-9Zn during melt spun process. Furthermore, the XRD patterns for solders containing 4 wt.% Al, indicate that the same phases of β-Sn and Zn are appeared additional to minor diffraction

ISSN 2347-3487

peaks observed for α-Al phase at 2θ = 38.67˚, and 44.98˚. The Al phase has face centered cubic structure. There is no any peak characteristic of an Al phase for 1, 2, 3. Wt.%, which means a complete solubility of Al in the Sn matrix. The lattice parameters a and c are calculated and the variation of the axial ratio (c/a) for β-Sn with the variation of Al compositions are listed in table 1. As indicated in Table1, the axial ratio increases to higher value 0.553 at 1 wt. % Al. The grain size is determined from the XRD pattern by using Scherrer's equation $D_{hkl}=0.891\lambda/\beta_{hkl}\cos\theta$, where D_{hkl} is the particle size, λ is the wavelength of Cu Kα =1.54056 Å, θ is the reflection angle and β_{hkl} is the breadth of the real line profile or full width at half maximum (FWHM) [17]. Addition of minor amount of Al refines the effective grain size while retaining uniform distribution of Al precipitates in the solidification process. The details of the x-ray diffraction analysis are shown in Table 1.

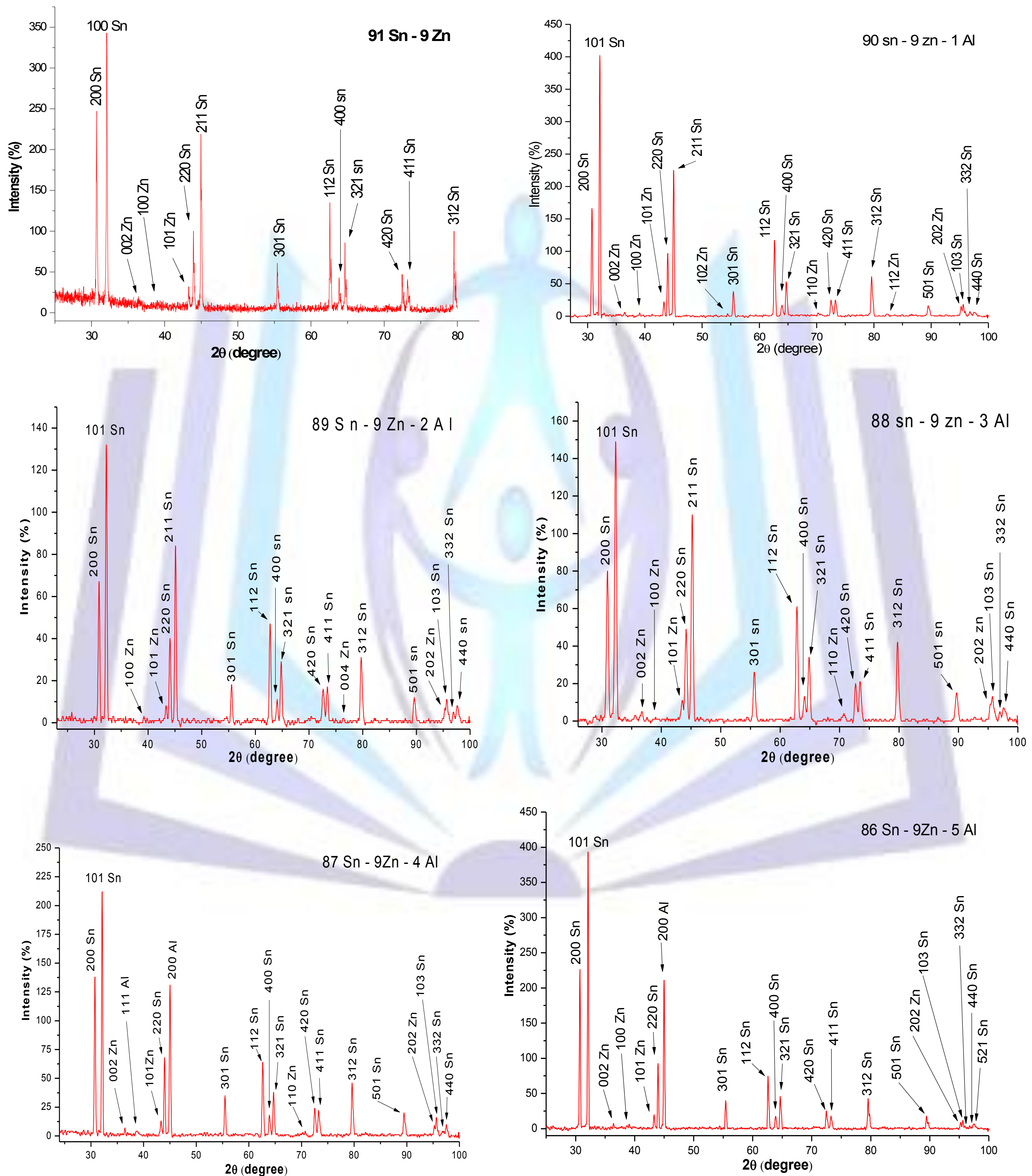

Fig.1. The x-ray diffraction (XRD) patterns Sn-9Zn-xAl (x=0, 1.0, 2.0, 3.0, 4.0 and 5.0 wt. %) solder alloys

ISSN 2347-3487

Table 1: The details of the XRD analysis

System	Phase designation	Crystal system	grain size (nm)	Typical parameter at concentration given wt.% Al		
				a (Å)	c (Å)	c/a
Sn- 9Zn	β-Sn	Body centered tetragonal	681.94	5.820	3.183	0.547
	Zn	Hexagonal	640.00			
Sn- 9Zn-1Al	β-Sn	Body centered tetragonal	738.57	5.785	3.197	0.553
	Zn	Hexagonal	620.22			
Sn-9Zn- 2Al	β-Sn	Body centered tetragonal	486.01	5.795	3.180	0.548
	Zn	Hexagonal	580.22			
Sn-9Zn- 3Al	β-Sn	Body centered tetragonal	627.43	5.803	3.186	0.549
	Zn	Hexagonal	480.36			
Sn-9Zn- 4Al	β-Sn	Body centered tetragonal	750.12	5.819	3.178	0.546
	Zn	Hexagonal	420.55			
	Al	Face centered cubic	488.25			
Sn-9Zn- 5Al	β-Sn	Body centered tetragonal	780.73	5.819	3.187	0.546
	Zn	Hexagonal	360.23			
	Al	Face centered cubic	430.54			

3.2 Microstructure

As cast microstructures of Sn-9Zn-xAl (x= 0.0 to 5 wt. %) solders, are shown in Fig.2 (a-f). The microstructure of Sn-9Zn-xAl alloys consists of primary Sn grains, eutectic structure and Zn particles distributed in Sn- matrix. With trace amount of Al (1, 2, 3 wt.%) addition the grain size is finer than that of eutectic binary system Sn-9Zn. The higher Al content (4, 5 wt.%), leads to the much finer grain size, and the more uniform distribution. The uniform microstructure of Sn-9Zn-xAl is obtained when Al is added into eutectic Sn-9Zn system. This is due to the adsorption phenomenon during solidification process of an alloy [31]. The finer and more homogeneous microstructure can have a favorable effect on the mechanical properties of the solder.

ISSN 2347-3487

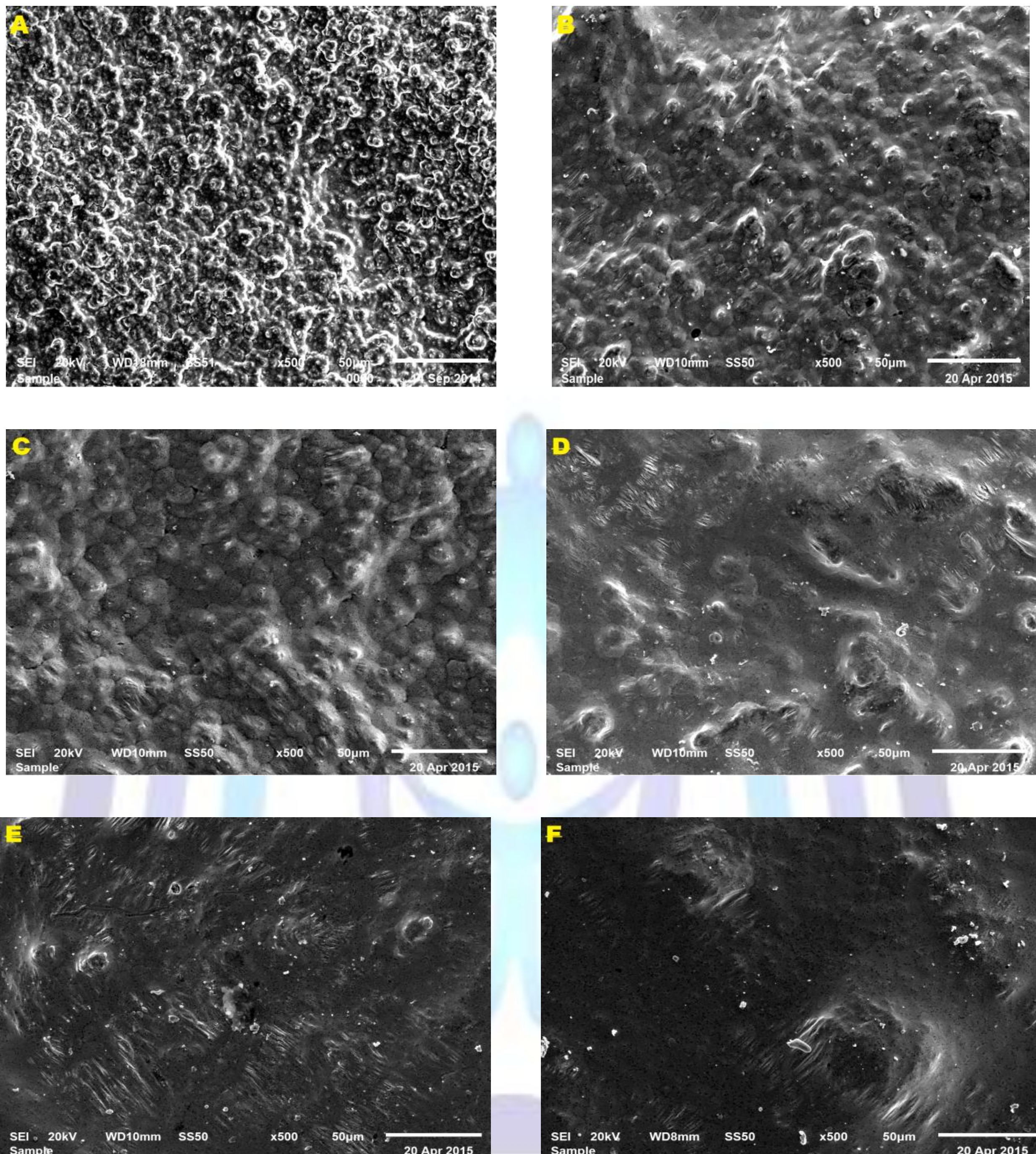

Fig.2 SEM microstructure of melt spun Sn-9Zn-xAl (x=0, 1.0, 2.0, 3.0, 4.0 and 5.0 wt. %) solder alloys

3.3 Melting Properties

Melting temperature is a critical solder characteristic because it determines the maximum operating temperature of the system. The melting properties of the melt spun ribbons were analyzed by DSC and the results are shown in Fig.3. Fig.3 shows single exothermic peaks corresponding to the melting of the binary eutectic Sn-9Zn and ternary Sn-9Zn-Al solder alloys during heating at rate of 10 ˚C/min. The melting points of the all melt spun alloys are derived from the corresponding melting peaks and shown in the Fig.3. The melting temperature of eutectic Sn-9Zn alloy found to be 198.43 C compared with literature value. Sharp exothermic peaks observes at 195.27 C in case of alloy containing 4 wt.% Al, the peak gradually broadened and shifted to lower temperature. This clearly indicates that the surface effects contributed in lowering the melting temperatures may be due to decrease in grain size. The pasty range, melting temperature, enthalpy of fusion, specific heat and entropy change of all solder alloys are given in Table 2.

ISSN 2347-3487

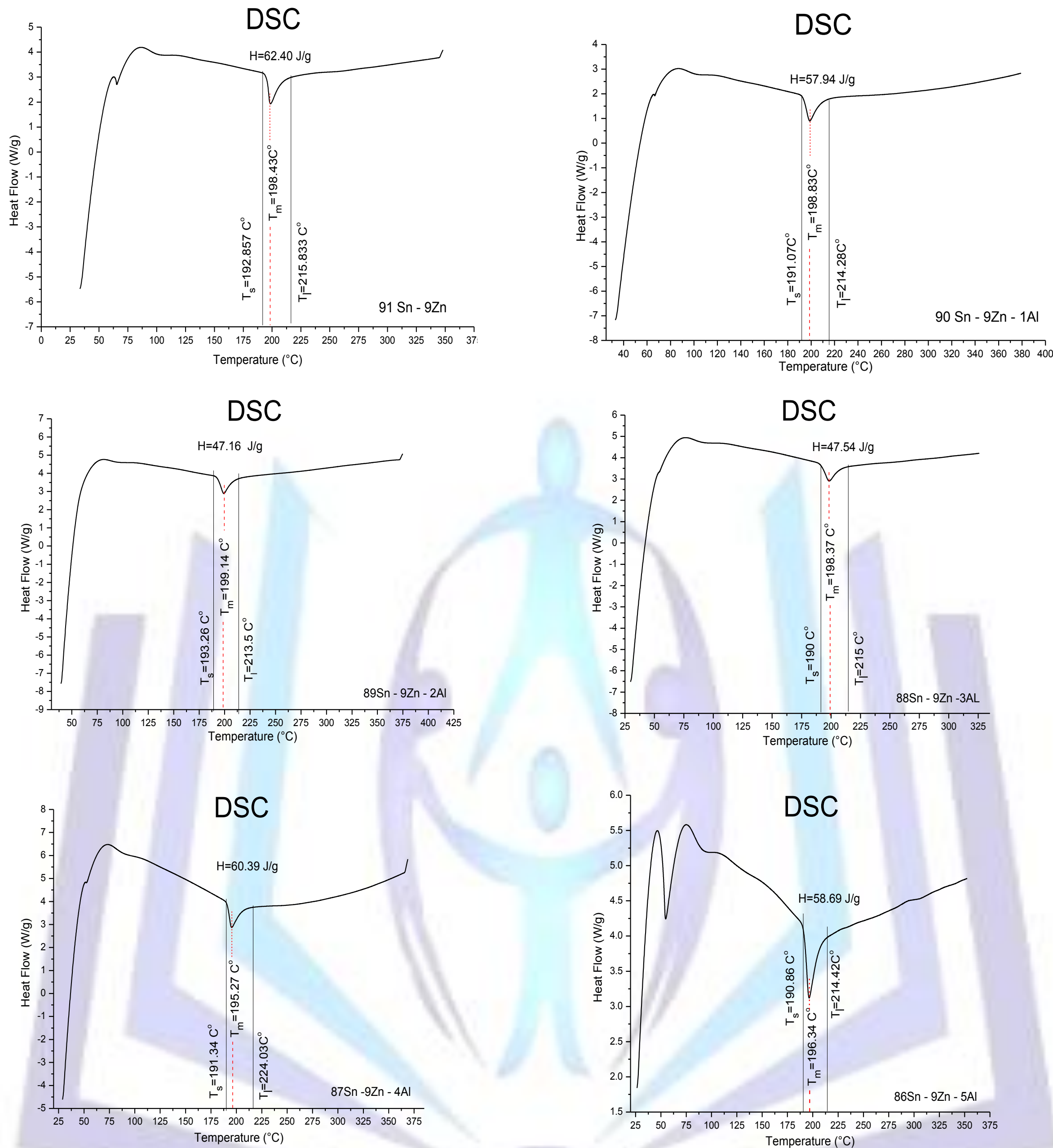

Fig.3. DSC curves of a Sn-9Zn-xAl (x=0, 1.0, 2.0, 3.0, 4.0 and 5.0 wt. %) solder melt spun alloys

Table 2: Melting analysis for all melt spun alloys including melting temperature, pasty range, specific heat, enthalpy and entropy change

Solder	Melting point (^{o}C)	Pasty range (^{o}C)	C_P (J/g.k)	Enthalpy ΔH (j/g)	ΔS Entropy change (j/g.k)
91Sn- 9Zn	198.43	0.0	2.7159	62.40	130.77
90 Sn – 9 Zn – 1 Al	198.83	23.21	2.4959	57.94	121.851
89 Sn – 9 Zn – 2 Al	199.14	20.23	2.3311	47.16	99.028
88 Sn – 9 Zn – 3 Al	198.37	25.00	1.9016	47.54	100.020
87 Sn – 9 Zn – 4 Al	195.27	32.69	1.8472	60.39	125.703
86 Sn – 9 Zn – 5 Al	196.34	23.56	2.4913	58.69	123.438

3.5 Mechanical properties and electrical resistivity of the solder joints

There is a continuous effort to better improve and understand mechanical properties of solder joints aiming to increase reliability. One frequently utilized way to influence properties of solder joints is to alloy either metallization (conductor) or solders with small amounts of additional elements. The Vickers hardness and dynamic Young's modulus of Sn-9Zn-Al are given in Table 3. The variations of Hv with Al content for test load, 0.098 N and 10 sec. It is found that the higher value of Hv for Sn-9Zn-2 wt.%Al melt spun alloy. The Sn-9Zn-2 Al has very good hardness 461.5 Mpa which is higher than that most other lead free solders alloys. This increasing in Hv may be attributed to some precipitates from Al in sn matrix. The effect of aluminium additions on the dynamic Young's modulus are shown in Table 3. It is noticed that Young's modulus increased with increasing Al content. High values in Young's modulus about 33.56 GPa at 3 wt.% Al due to presence of some precipitates from Al element. The values of dynamic Young's modulus and Hv are substantially higher for Al additions than alloy free Al. This is attributed to dissolves of Al in Sn matrix. In microelectronic devices the solder serves as an electrical interconnection. The electrical resistivity (ρ) of as-quenched melt spun alloys is measured at room temperature and the results are shown in Table 3. The electrical resistivity increases with increasing aluminium content and gives the highest value of about $82.49x10^{-6}$ ohm.cm at 3 wt.% Al. Such a high electrical resistivity is considered to have been attained by the combination of several affects; the uniform distribution of fine precipitates the introduction of internal defects such as dislocations and the formation of the Al phase dissolves in Sn matrix. The Al atoms act as scattering centers in β-Sn matrix.

Table 3. Microhardness, dynamic Young's modulus and electrical resistivity

System	Hv MPa	Dynamic Young's modulus (GPa)	Electrical resistivity 10^{-6} Ω.cm
Sn-9Zn	227.5	44.342	33.65
Sn-9Zn-1.0 Al	322.0	32.736	36.45
Sn-9Zn-2.0 Al	461.5	29.897	82.02
Sn-9Zn-3.0 Al	388.0	33.564	82.49
Sn-9Zn- 4.0 Al	404.8	29.238	73.97
Sn-9Zn-5.0 Al	442.3	28.828	64.65

Conclusions

We have investigated experimentally the properties of Sn-Zn-Al solders as quenched ribbons from melt and found the following:

1. The addition of Al to Sn-9Zn eutectic alloy leads to the formation of body centered tetragonal Sn, hexagonal Zn and face centered cubic Al phases.
2. Addition of minor amount of Al to Sn-9Zn eutectic solder refined the grain size, in general case.
3. The ternary alloy Sn-9Zn-4 wt.% Al has the most suitable properties required for solder applications as a replacement of Sn-Pb eutectic alloy; it has a lower melting point 195 ˚C, which is close to that of Sn-Pb solder alloy.
4. The microhardness measurement is a powerful tool in the determination at the quality of alloys. It is also observed that the hardness of Sn-9Zn-2 wt.%Al is higher than that of the Sn-9Zn is due to refinement of precipitates in the solidification microstructure.
5. Effect of aluminum content reduced the Young's modulus and increased the electrical resistivity of the Sn-9Zn eutectic melt-spun ribbons as indicated in the Table 3. It is concluded that the eutectic composition of Sn-9Zn is the best for electrical resistivity, 33.65 μΩ.cm and Young's modulus, 44.34 GPa with comparison of Sn-Zn-Al ternary system.

References

1. M.kamal, S.Gouda and R.M. Shalaby , Effect of small additions of Ag, Bi, Cu and Sb on structure and solder properties of Sn-Zn eutectic alloy , Acta Ciencia Indica,Vol. XXXVIII P. No,2 141 (2012).
2. Gomidzelovic L, Zivkovic D, Kostov A, Mitovski A, Balanovic L. Comparative thermodynamic study of Ga-In-Sb system. J Therm Anal Calorim. 2011; 103: 1105-9.
3. Amore S, Delsante S, Parodi N, Borzone G. Calorimetric investigation of the Cu-Sn-Bi lead free solder system. J Therm Anal Calorim. 2008; 92: 227-32.
4. Tomasz Gancarz, Przemyslaw Fima, Janusz Pstrus, JMEPEG (2014) 23: 1524-1529.

5. M.L.Huang, X.L.Hou, N.Kang, Y.C.Yang , J Mater Sci: Mater Electron (2014) 25: 2311-1319.
6. Rizk Mostafa Shalaby , Cryst. Res. Technol. 45, No. 4, 427 – 432 (2010) / DOI 10.1002/crat.201000022.
7. L.Zhang, S.Xue, L.Gaw, Z.Sheng, and H.Ye, Development of Sn-Zn lead free solders bearing Alloying elements, J.Mater.Sci.:Mater.Electron., 2010, 21(1), p 1-15.
8. M.McCormack , S.Jin, H.S.Chen, and D.A.Machusak, New lead-free Sn-Zn-In solder alloys, J.Electron. Mater. , 1994, 23(7) , p 687-690.
9. T.C.Chang, M.H.Hon, M.C.Wang, J.AlloysCompd.352 (2003)168-174.
10. J.M.Song, T.S.Lui, G.F.Lan, L.H.Chen, J.Alloys Compd. 379(2004)233-239.
11. K.I.Chen, S.C.Cheng, S.Wu, K.L.Lin, J. Alloys Compd. 416 (2006)98-105.
12. J.w.Yoon, S.B.Jung, J AlloysCompod. 407 (2006)141-149.
13. K.S.Kim, J.M.Yang, C.H.Yu, I.O.Jung, H.H.Kim, J.Alloys Compod.381 (2004)314-318.
14. L.L.Duan, D.Q.Yu, S.Q.Han, H.T.Ma, L.Wang, J.Alloys Compod. 381 (2004)202-207.
15. J.W.Yoon, S.B.Jung, J.Mater.Res. 21 (2006) 1590-1599.
16. T.El-Ashram and R.M.Shalaby, Electron. Mater. 34, 212 (2005).
17. B.D.Cullity; Elements of X-ray Diffraction, 2nd Edition,Addison-Wesely Publishing Company ,pp.248,(1978).
18. M.Kamal, A.M.Shaban, M.El-Kady and R.M.Shalaby, "Irradiation, mechanical and structure behavior of aluminium-zinc based alloys rapidly quenched from melt", Radiation Effects and Defects in Solids,Vol.138, pp.307-318, 1996.
19. Kamal, A.M.Shaban, M.El-Kady and R.M.Shalaby, "Determination of structure –property of rapidly quenched aluminium-based bearing alloys before and after gamma irradiation", 2nd International Conference of Engineering Physics and Mathematics, Faculty of Engineering, Cairo University, Cairo, Vol.2, pp.107-121, 1994.
20. Rizk Mostafa Shalaby, Mohammed Younus, Abu-Bakr El-Bediwi, Mustafa Kamal, "Correlation between microstructure, mechanical and thermal properties of In-Bi-Sn-Ag melt spun alloys" JOURNAL OF ADVANCES IN PHYSICS Vol.8, No.1, March, (2015) 2022-2042.
21. Mustafa Kamal, Abu-Bakr El-Bediwi, *Rizk Mostafa Shalaby*, Mohammed Younus ," A study of eutectic indium-bismuth and indium-bismuth-tin Field's metal rapidly solidified from melt " JOURNAL OF ADVANCES IN PHYSICS Vol.7, No.2, January , (2015) 1404-1414.
22. Mustafa Kamal and Usama S. Mohamed, A Review Chill-Block Melt spin Technique, Theoretical and Applications, EISBN: 978-1- 608005-151-9(2012), Bentham eBooks.
23. H. H. Liebermann, Materials Science and Engineering, 43 (1980) 203-210.
24. Y.A.Geller, A. G. Rakhshtadt,"Science of Materials, Mir publishers, Moscow, 1977, P. 138.
25. A.M. Shaban and M. Kamal, Radiation Effects and Defects in Solids, (1995), Vol.133, PP: 5-13.
26. Mustafa Kamal and Abu-Baker El-Bediwi, Radiation Effects and Defects in solids 174(1999)211.
27. Whetten R.L., Khoury J.T., Alvarez M.M., Murthy S., Vezmar I., Wang Z.L., Stephens P.W., Cleveland C.L., Luedtke W.D.and Landman U., Nanocrystal gold molecules;Advan. Mater; 1994; 8: 428-433.
28. Murray C.B., Kagan C.R. and Bawendi M.G., Self-Organization of CdSe Nanocrystallites into Three-Dimensional Quantum Dot Superlattices; Scienc; 1995; 270: 1335-1338.
29. Murray C.B., Kagan C.R. and Bawendi M.G., Synthesis and Characterization of Monodisperse Nanocrystals and Close-Packed Nanocrystal AssembliesAnn. Rev. Mater. Sci.; 2000; 30: 545-610.
30. Alivisatos A.P., Semiconductor clusters, nanocrystals, and quantum dotsScience ; 1996; 271:933-937.
31. D.Q Yu, J.Zhao, L.Wang, Journal of Alloys and Compounds 376(2004)170-175.